Constellation-X Mirror Technology Development

W. W. Zhang, J. Bolognese, G. Byron[3], K.W. Chan[1], D.A. Content, T.J. Hadjimichael[2], Charles He[2], M.D. Hill, M. Hong[3], J.P. Lehan[1], L. Lozipone[3], J.M. Mazzarella[3], R. McClelland[3], D.T. Nguyen, L. Olsen[3], R. Petre, D. Robinson, S.O. Rohrbach, R. Russell[3], T.T. Saha, M. Sharpe[3]
NASA Goddard Space Flight Center
[1] also University of Maryland, Baltimore County
[2] Ball Aerospace and Technologies Corp.
[3] Stinger Ghaffarian Technologies, Inc.

M.V. Gubarev, W.D. Jones, and S.L. O'Dell
NASA Marshall Space Flight Center

W. Davis, D.R. Caldwell, M. Freeman, W. Podgorski, and P.B. Reid
Smithsonian Astrophysical Observatory

ABSTRACT

As NASA's next major space X-ray observatory, the Constellation-X mission (Bookbinder et al. 2008) requires mirror assemblies with unprecedented characteristics that cannot be provided by existing optical technologies. In the past several years, the project has supported a vigorous mirror technology development program. This program includes the fabrication of lightweight mirror segments by slumping commercially available thin glass sheets, the support and mounting of these thin mirror segments for accurate metrology, the mounting and attachment of these mirror segments for the purpose of X-ray tests, and development of methods for aligning and integrating these mirror segments into mirror assemblies. This paper describes our efforts and developments in these areas.

Keywords: X-ray optics, lightweight optics, Constellation-X, space optics

1. INTRODUCTION

We adopt the traditional Wolter-I optical design: parabolic primary mirrors and hyperbolic secondary mirrors. It is well suited for nesting many shells to achieve large effective areas. For the convenience of discussion, the standard parabolic or hyperbolic prescription of a mirror can be described in the coordinate system as shown in Figure 1 as follows

$$\rho(z,\phi) = \rho_0 + \Delta\rho(\phi) + z\cdot\tan[\theta_0 + \Delta\theta(\phi)] - \left(\frac{2z}{L}\right)^2 \cdot [s_0 + \Delta s(\phi)] + R(z,\phi),$$

$$0 \le \phi \le \phi_{\max}, -\frac{L}{2} \le z \le \frac{L}{2},$$

where ρ_0, by definition, is azimuth-independent, is the *average radius*; $\Delta\rho(\phi)$ is *radius variation* as a function of azimuth, characterizing any circularity error; θ_0, by definition, is azimuth-independent, is the *average cone angle*; $\Delta\theta(\phi)$ is *cone angle variation*, commonly also referred to as the $\Delta\Delta R$ error; s_0, by definition, is azimuth-independent, is the *average sag*; $\Delta s(\phi)$ is sag variation as a function azimuth; the

Space Telescopes and Instrumentation 2008: Ultraviolet to Gamma Ray, edited by Martin J. L. Turner,
Kathryn A. Flanagan, Proc. of SPIE Vol. 7011, 701103, (2008) · 0277-786X/08/$18 · doi: 10.1117/12.788453

last term $R(z,\phi)$, or the *remainder*, represents the rest of the description; the parameter L (=200mm) is the axial height of the mirror shell or segment.

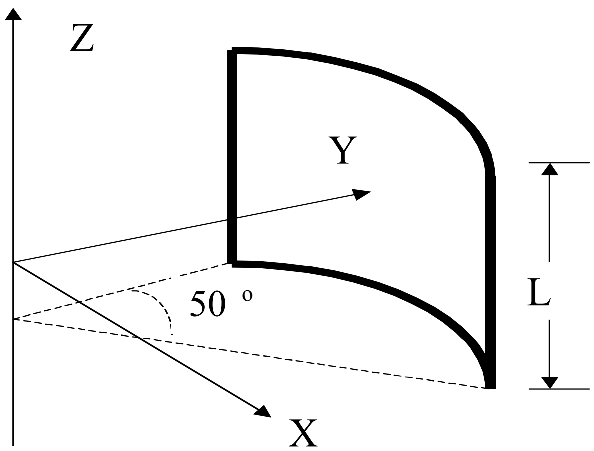

Figure 1. Coordinate system used to describe the mirror segment.

For all intents and purposes, a mathematically perfect mirror, parabolic or hyperbolic, has not azimuth-dependent terms nor the remainder. (Mathematically Wolter-I mirrors do have third order terms, but they are so small that we can safely neglect them when working in the context of a mirror that is far from the diffraction limit.)

For this mirror technology development, we have made two strategic decisions from the outset. The first one is that we have adopted a segmented design and scalable implementation, as opposed to the whole shell design and implementation used by the Chandra and XMM/Newton observatories. This is to ensure that the techniques we develop, at least in principle, can be used to design and construct arbitrarily large mirror assemblies to meet the need of X-ray astronomy for large photon collection areas. The second one is that we adopted the original Wolter-I design, as opposed to conical approximations. This decision means that the ultimate angular resolution of the telescope will be limited by mirror fabrication errors and alignment errors, not by the limit of the optical design as is the case if one uses a conical approximation of the Wolter-I design.

Our development program is partitioned into four steps: (1) mirror segment fabrication, (2) mirror segment metrology, (3) temporary mounting of the mirror segment, and (4) permanent mounting of the mirror segment. On the one hand, these steps are interrelated with and depend on each other for making progress. On the other hand, each step can be developed to one degree or another independently of other steps. The efficiency and the speed of our technology development lie in the wise management of these steps. In the following sections we describe the purposes and status of each of these four steps.

2. MIRROR SEGMENT FABRICATION

The mirror segment fabrication is a three-step process: (1) slumping, (2) post-slumping cutting or trimming, and (3) coating. The process starts with commercially available thin (0.4mm) glass sheets, either Schott D263 or AF45. These glass sheets are placed atop a precision-figured forming mandrel whose surface has been conditioned to prevent sticking, as shown in Figure 2. They are heated in an oven to ~600^0C gradually so that the glass sheet becomes soft and sags under its own weight and wraps itself around the mandrel, taking its accurate shape. The glass sheet is then properly annealed and cooled to room temperature.

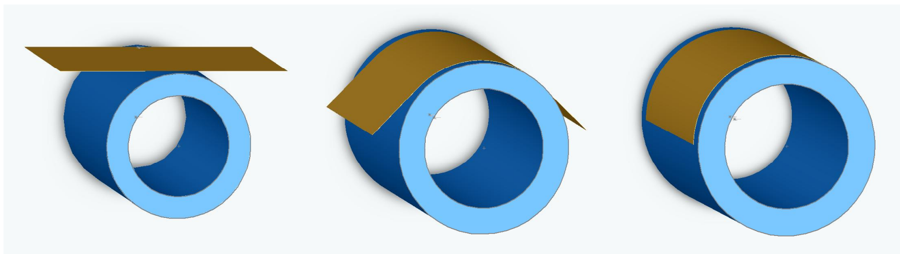

Figure 2. An illustration of the mirror forming process. The whole process takes place inside an electric oven meeting stringent temperature uniformity requirements.

The second step of the fabrication process takes place after the glass sheet has cooled to room temperature. It is cut to a prescribed size meeting requirements for integration into a precision housing. Another important function of this step is to remove the areas near the edges which typically do not conform accurately to the mandrel because of gravity and thermal effects. A hot-wire technique is used for this cutting to ensure that the resulting edges are free of factures which can propagate and result in mirror breakage.

The last step of the mirror fabrication is to coat the inner (or concave) surface with approximately 15nm of iridium to enhance its x-ray reflectivity. In principle, any number of metals could serve this purpose. But iridium is especially desired for its highest x-ray reflectivity for x-rays around 6 keV. Iridium is a noble metal with a very high melting point. In general its coating tends to create compressive stress that can distort the figure of the mirror segment. Part of our investigative effort is to minimize or even eliminate any stress associated with Ir coating.

3. MIRROR SEGMENT METROLOGY

The function of mirror segment metrology is to measure its intrinsic figure. It has two important purposes. The first one is providing feedback to the mirror fabrication process so that it can continue to improve its quality. The second purpose is providing a benchmark or standard for the later steps of mirror mounting and alignment.

Mirror segment metrology poses two challenges. The first one pertains to the flexibility of the mirror segment in question: an aspect ratio of 200mm over 0.4mm or 500. It distorts easily under its own weight and by any inadvertent handling or frictional forces. The second one pertains to the cylindrical nature of x-ray optics. Nearly all commercially available metrology tools are designed and made for nearly planar mirrors which have nearly plane or spherical wave fronts.

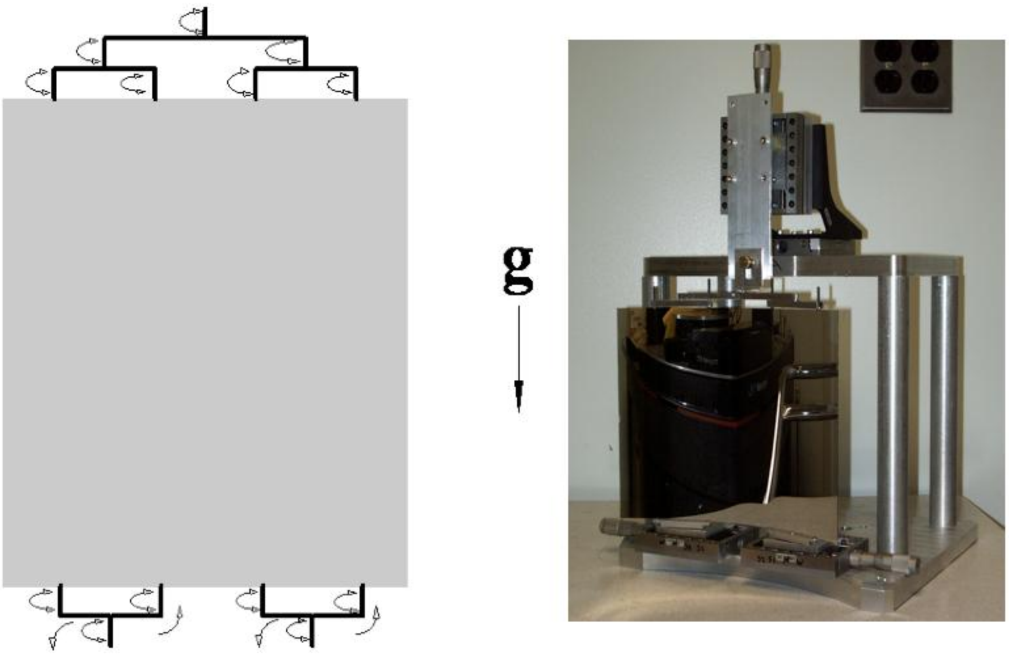

Figure 3. An illustration of the Cantro-tree concept (left panel) and a photo of a laboratory implementation (right panel).

Figure 4. An illustration of the suspension mount (left panel) and a photo of a laboratory implementation (right panel). Note that the two strings hanging the mirrors are very long to minimize any horizontal component of their tensions which can distort the mirror.

We have developed two methods to meet the first challenge. The first one is the Cantor-tree, similar to the whiffle-tree commonly used for supporting normal incidence optics. As shown in Figure 3, the Cantor-tree holds a mirror in the vertical or nearly vertical configuration. The branches of the Cantor-tree are connected with bearings that move freely to minimize any stress on the mirror segment. The Cantor-tree performs two functions: (1) supporting the mirror with minimal distortion and (2) preventing the mirror from freely vibrating by air currents that inevitably exist in a typical laboratory environment. See Lehan et al. (2008) for more details.

The second one is a mount based on suspending a mirror segment using two strings. The concept and a laboratory implementation are shown in Figure 4. The suspension is such that the center of gravity of the mirror segment and the two suspension strings are in the same vertical plane, minimizing any potential distortion caused by gravity torques. While the mirror is suspended, a strongback that is made of the same type of glass as the mirror segment is attached to the back of the mirror with four accurately adjusted standoffs. These standoffs are dabbed with small beads of epoxy for bonding. After the epoxy cures, the two strings are cut and the mirror segment is handled through the strongback. See Chan et al. (2008) for more details.

The actual measurement of the mirror segment is performed using a 10-in aperture Fizeau interferometer and a cylindrical lens which converts a plane wave into a cylindrical wave, as shown in Figure 5.

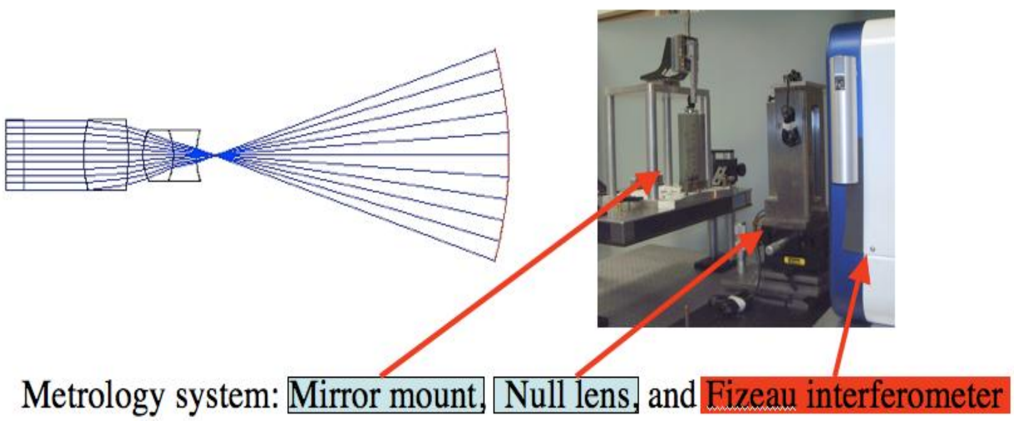

Figure 5. An illustration of the whole surface interferometric measurement system (left) and the actual laboratory setup.

Several mirror segments have been measured multiple times separately on the Cantor-tree mount and on the suspension mount. Excellent repeatability has been achieved separately for them and excellent agreement has been achieved between the two rather independent ways of mounting the mirror. Figure 6 shows two separate measurements of the same mirror: one on the Cantor-tree and the other on the suspension mount. Qualitatively the measurements are very similar, but quantitative differences are apparent. The cone angle variation vs. azimuth curves (top panels) show that the suspension mount seems to have larger magnitudes. This is not surprising since the mirror segment is bonded at four points and therefore overconstrainted on the suspension mount, whereas it is “free-floating” on the Cantor-tree mount. Another systematic difference is in the average sag values between the two. Typically the average sag measured of a mirror on the Cantor-tree is about 0.25µm larger than that measured on the suspension mount. It is possible that the difference between a mirror sitting on its end vs. the same mirror being hung from two strings. This systematic difference will be studied both experimentally and numerically in the next year.

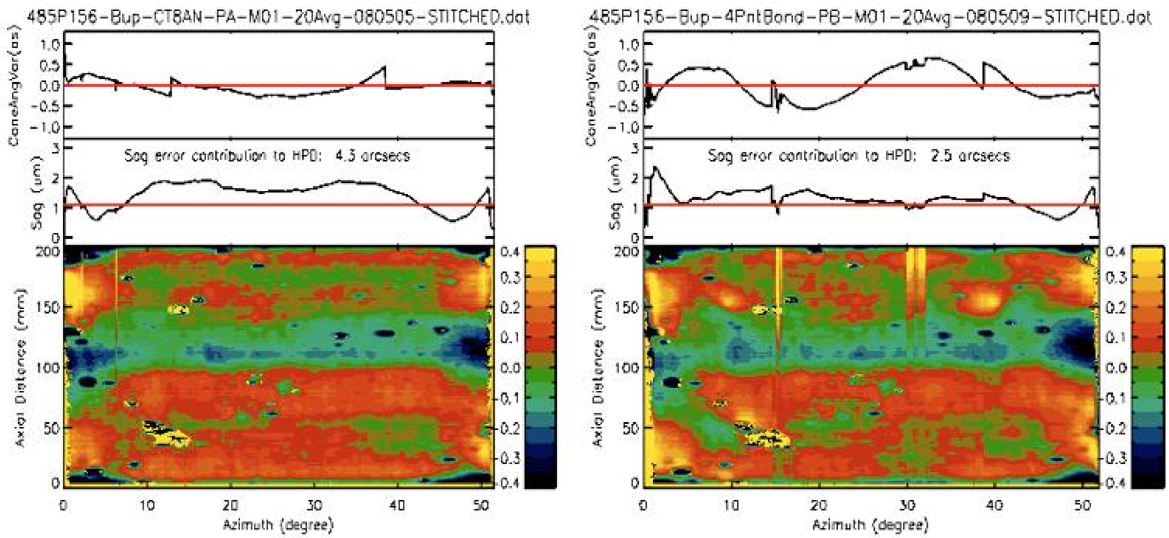

Figure 6. Comparison of two measurements of a mirror segment (485P156). For the first measurement (left) the mirror was supported by the Cantor-tree mount. For the second (right) it was on the suspension mount. The top panels plot the cone angle variation vs. azimuth; the middle panels the sag variation vs. time. The color topograph at the bottom represents the remainder, the color scale being in μm.

4. TEMPORARY MOUNTING OF THE MIRROR SEGMENT

The next step of the process is to mount mirror segments temporarily as an intermediary step to mounting them permanently into a housing. In this step, the mirror segment is temporarily attached or bonded to a rigid structure and becomes effectively a rigid body that can be handled and aligned using conventional techniques and tools. A very important byproduct of this step is that the mirror segments can be aligned in their temporary mounts and placed in an x-ray beam for full-illumination tests, verifying definitively the metrology results and the alignment process.

We have been developing in parallel three ways of accomplishing the temporary mounting: (1) the optical alignment pathfinder (OAP), (2) cradle and mattress, and (3) suspension mount as described in the last section.

The OAP uses ten adjusters, five at the forward edge and five at the aft edge, to hold the mirror such that its optical axis is in the vertical direction. The ten adjusters can adjust the mirror segment in their local radial directions, changing the mirror average radius and cone angle (Reid et al. 2008). In this sense, OAP represents an active approach. It is likely that, when the adjustment is finished, the mirror segment has a different figure and parameters from their intrinsic ones. For details and status of the OAP approach, see Podgorski et al. (2008).

The cradle and mattress system seeks to negate the effect of gravity using many very soft springs. In this scenario, the optical axis of the mirror segment in question is actually nearly horizontal. Individual rows of springs are adjusted such that the mirror segment achieves the best possible figured as defined by a grazing incidence Hartmann map made up of points measured of different azimuthal positions. Then the mirror segmented is bonded at several points along its two azimuthal sides. A pair of mirrors have been successfully bonded and aligned this way and have been placed in an x-ray beam. Figure 7 shows the test results. For more details and status of the cradle-mattress approach, see Hadjimichael et al. (2008) and Rohrbach et al. (2008).

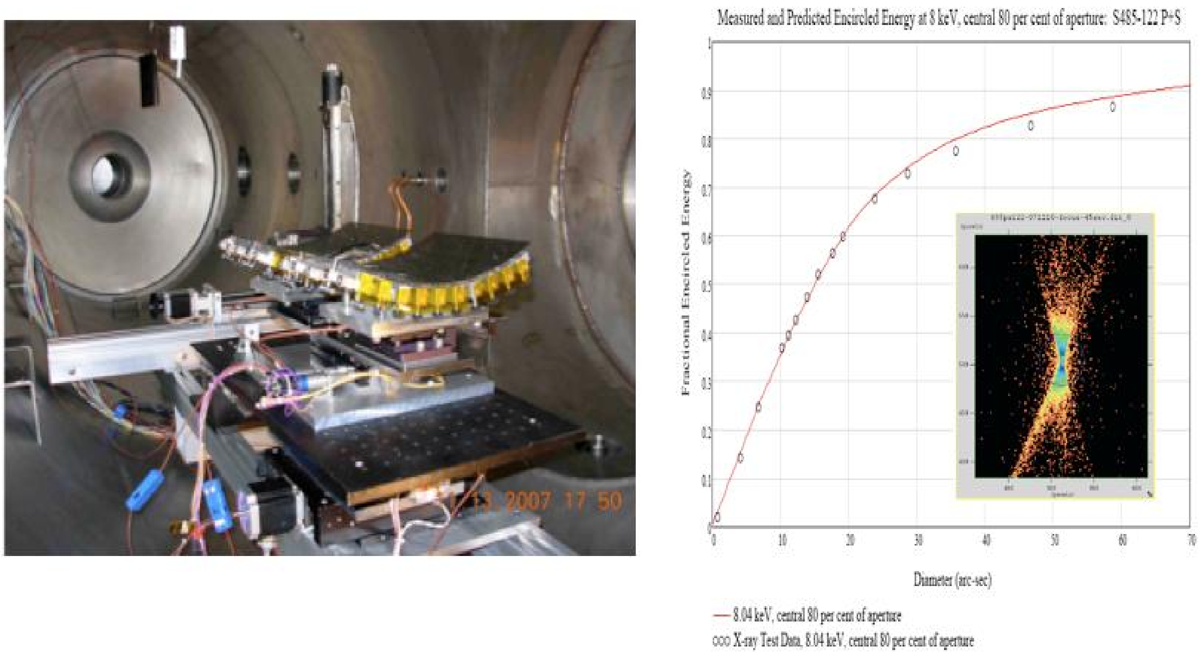

Figure 7. A pair of mirrors on the cradle-mattress system placed in a vacuum chamber ready for full-illumination x-ray test (left). The resulting fractional encircled energy vs. image diameter (right) and the actual x-ray image (inset).

The third approach is the suspension mount as described in the last section. Its advantage is that the mirror segment is already bonded to a strongback. In order to be x-ray tested, it needs to be turned 90 degrees such that it optical axis is horizontal as the x-ray beam is horizontal. Optimization can be performed to position the four bond points so that the distortion in the “smile” configuration is minimized. As of the writing of this paper, we are preparing a pair of mirrors in this configuration for a full-illumination x-ray test.

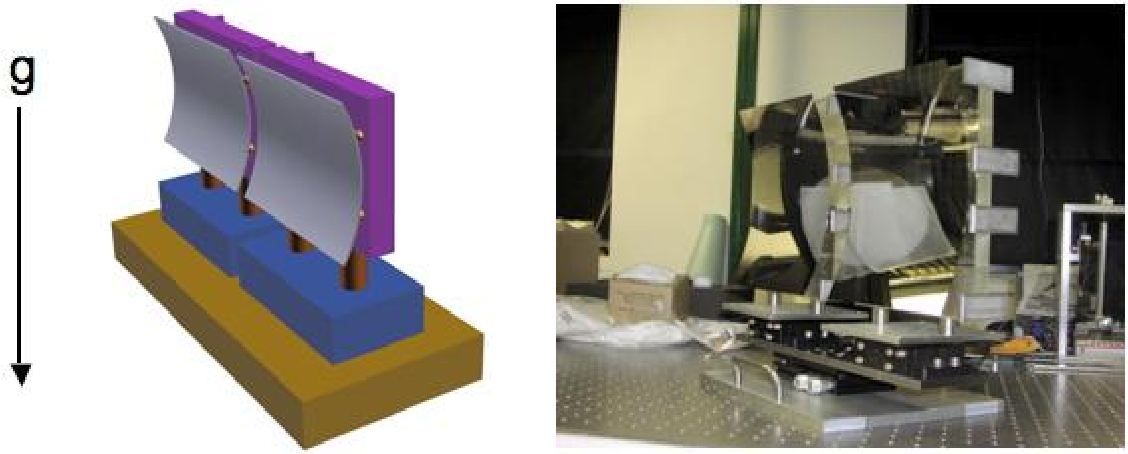

Figure 8. Illustrations of suspension-mounted mirrors prepared for x-ray test in an x-ray beam (left). A laboratory implementation of the concept is also shown (right). The mirror segments as mounted are rotated 90 degrees such that their optical axis is horizontal.

5. PERMANENT MOUNTING: ALIGNMENT AND INTEGRATION

The next step of the process is to transfer the mirror segment from the temporary mount to a permanent housing to form a module. The step starts with the temporarily mounted mirror segment being manipulated into the correction configuration as defined by the optical design and aligned to focus to the system focus. It is then bonded at a number of points along its edges. When the adhesive cures, the mirror segment is released from the temporary bonding points. We are investigating different methods of bonding the mirror segment: (1) single-sided bonding, (2) double-sided bonding, and (3) bonding with or without a precision reference surface. We are too early in the process to report definitive conclusions as to which one of these would work the best.

6. SUMMARY AND OUTLOOK

We have adopted a systematic approach for the Constellation-X mirror technology development. Each step of the process is well-defined with clear objectives and ways to achieve them. We have met the mirror requirements of 15” HPD in the areas of mirror fabrication and metrology. We are in the process of developing adequate ways of permanently mounting mirror segments into a module housing. In this section, we will take a quantitative look at the status of mirror fabrication and metrology and define what errors need to be reduced in order to achieve the 5” HPD goal of the mission.

Table 1 lists the mirror quantities that were introduced in the Introduction section at the beginning of this paper. The contribution of each quantity to the image half-power diameter is also listed.

Table 1. Mirror segment quality status and their prospects of reaching the 5" HPD goal. At present mirror pairs perform at the 10" level which is adequate for a 15" mirror assembly. The enabling of a 5" mirror assembly requires mirror pars performing at the 4" level or better.

		Now			Future		
Quantity		Potential Source of Error	Existing Evidence ?	Contribution to HPD (")	Method to Reduce or Eliminate Error	Contribution to HPD after Mitigation (")	Comment
Radius	Average Radius	CTE mismatch between mandrel and glass sheet	No	0	Account for CTE mismatch in mandrel prescription	0	Easy
	Radius Variation	Gravity distortion	No	0	Improve mirror support mechanism	0	Moderately hard
Cone Angle	Average Cone Angle	Forming mandrel	Yes	0	Obtain better mandrel	0	Easy
	Cone Angle Variation	Gravity distortion	Yes	0	Improve mirror support mechanism	0	Moderately hard
Sag	Average Sag	Gravity distortion	Yes	1	Improve mirror support mechanism	0	Moderately hard
	Sag Variation	Coating stress	Yes	5	Reduce or eliminate coating stress; Balance coating stress	0	Maybe easy
Axial figure	Low frequency figure	Forming mandrel	Yes	5	Obtain better mandrel	2	Easy
	Mid frequency figure	Forming mandrel	Yes	2	Obtain better mandrel	1	Easy
		BN-coating changing mandrel figure	Yes	7	Improve release layer smoothness; RF-sputter; Reactive sputter	3	Hard
	High frequency figure	Glass sheet quality	Yes	2	Super-polish glass sheets if necessary	2	Moderately hard
Mirror Pair Performance HPD (")				10		4	

Average radius: In combination with the average cone angle, the average radius determines the focal length. Currently we have not yet definitively measured the average radius. Although we believe that the average radius, at worst, will have some systematic shift from prescription, we will invest effort on its definitive measurement in coming months. When only a single shell is concerned, it does not contribute to the final image quality because any error can be removed by changing the detector position.

Radius variation: We have measured radius variation, or non-circularity, of mirror segments using a transmission sphere that converts a plane wave to a spherical wave. We have found that the mirror segments are remarkably circular. The typical deviation is on the order of 1μm or less. Given the grazing nature of x-ray optics, this error does not contribute to the degradation of the image quality.

Average cone angle: In combination with the average radius, the average cone angle determines the focal length. At present we have not yet definitively measured this quantity. We will invest efforts to measure this quantity in coming months.

Cone angle variation: This error of the mirror segment as fabricated is quite small. But we have noticed that it can easily be introduced in the mounting and bonding process.

Average sag: Currently we have observed systematic errors in measuring the average sag at the 0.25μm level. This systematic error is negligible for a 15" mirror system, but is a significant factor for a 5" system. We need to reduce this uncertainty to ~0.05μm level.

Sag variation: This error is the second largest contributor to the final image quality. There is strong evidence that this variation is caused by the Ir coating stressing the glass substrate. We will investigate different ways of applying the Ir coating and expect to reduce this error to negligible levels.

Low frequency figure: The entire amount of error comes from the forming mandrel quality. In other words, the slumping process accurately copies the figure of the forming mandrel in this spatial frequency regime. We will procure better forming mandrels to reduce this error term.

Mid-frequency figure: This error comes from two sources: the forming mandrel itself and, more importantly, the BN-release layer which tends to change the figure of the mandrel in this regime. This error also is the largest contributor to the image quality. We expect further work in the BN-release layer coating process will reduce this error by more than a factor of 2.

Microroughness: This is determined by the float glass sheets themselves. This is a negligible error.

In a nutshell, in order to reach the 5” goal, we need to significantly reduce the mid-frequency error: by a factor ~3. We also need to procure better forming mandrels. In the metrology area, we need to understand and substantially reduce the systematic error in measuring the average sag. We also need to better understand the coating process to significantly reduce the coating stress while preserving the microughness.

REFERENCES

1. Bookbinder J. et al., 2008, in these proceedings
2. Reid, P. B. et al., 2008, in these proceedings
3. Chan, K.W. et al., 2008, in these proceedings
4. Lehan, J.P., et al., 2008, in these proceedings
5. Hdajimichael, T. et al., 2007, in these proceedings
6. Rohrbach, S. et al. 2008, in these proceedings
7. Zhang, W.W. et al., 2007, Proc. SPIE, Vol. 6688, p. 668802